ASTRONOMY & ASTROPHYSICS
SUPPLEMENT SERIES

MARCH II **2000**, PAGE 373

Astron. Astrophys. Suppl. Ser. **142**, 373–387 (2000)

Kinematics and CMD of the globular cluster NGC 4147

J.J. Wang[1,2,3], **L. Chen**[1,2], **Z.Y. Wu**[1,2], **A.C. Gupta**[4,5,6], **and M. Geffert**[7]

[1] Shanghai Astronomical Observatory, CAS, Shanghai 200030, PR China
[2] National Astronomical Observatory, CAS, Beijing 100080, PR China
[3] Joint Laboratory for Optical Astronomy, CAS, Shanghai 200030, PR China
[4] Department of Physics, University of Gorakhpur, Gorakhpur 273 009, India
[5] U. P. State Observatory, Manora Peak, Nainital 263 129, India
[6] Physical Research Laboratory, Navarangpura, Ahmedabad 380 009, India
[7] Sternwarte der Universität Bonn, Auf dem Hügel 71, D-53121 Bonn, Germany

Received May 6; accepted December 9, 1999

Abstract. Astrometry and $BVRI$ CCD photometry of 115 stars down to $B = 17.6$ in the region of about $11' \times 11'$ around the globular cluster NGC 4147 was performed. In the astrometric reduction, three earlier epoch plates taken at Sheshan, Shanghai, China, in 1958 and four recent epoch B-passband CCD frames taken at Kavalur, India, were used. The data were reduced to a catalogue based on measurements of stars on seven plates with an epoch period from 1917 to 1979 taken in Bonn, Germany, and ultimately to the Hipparcos catalogue. The reduction was done with the central overlapping method. Based on the new proper motion data, the membership probabilities of 115 stars were determined. Furthermore, three colour-magnitude diagrams (CMD) of V versus $B-V$, $V-R$ and $V-I$, respectively, for HB and GB stars were constructed from CCD photometry obtained with the Vainu Bappu Telescope. An absolute proper motion of the cluster of -2.08 ± 0.48 mas/yr in right ascension and -3.07 ± 0.46 mas/yr in declination has been obtained. The space velocity and apogalactic distance of the cluster with respect to the Galactic standard of rest were calculated. In contrast to the first results given in the literature we obtain a significantly lower velocity and a smaller apogalactic distance for NGC 4147.

Key words: stars: kinematics — stars: Hertzsprung-Russell and C−M diagrams — globular clusters: individual: NGC 4147

1. Introduction

Globular clusters (GCs) are among the oldest stellar objects in the Milky Way. Due to the total luminosity from the large number of stars, they can be observed far away. They play very important rôles in the study of the structure and evolution of the Galaxy. For instance, with GCs as a new constraint, Dauphole & Colin (1995) studied the mass distribution in our Galaxy, re-calculated the model potential and obtained a better consistency with the observations. The formation of the Galaxy was studied by Eggen et al. (1962; hereafter ELS), which were in favour of a pressure supported rapid collapse model (ELS model), while Searle & Zinn (1978; hereafter SZ) proposed an accretion model of Galaxy formation (SZ model). Their model is based on the fact that the globular clusters could be considered as relics of some sub-systems merging with the Galaxy, these relics still having different kinematics and metal abundances. Geffert et al. (1995) and Dauphole et al. (1996), using a sample of 26 GCs with absolute proper motion data, found a correlation between the apogalactic distances and the metallicities in support of the ELS model.

Kinematic parameters of globular clusters may provide important information for the understanding of the formation of the Galaxy. The reliability of their determination, however, depends of the quality of the proper motion measuring. In fact, the accuracy of radial velocities of the GCs, at present, is better than ± 1 km s^{-1} and the accuracy of distance determination is better than 10%. On the other hand, if the proper motion accuracy were ± 1 mas/yr –a typical value for a recent proper motion determination– it would lead to an uncertainty of 50 km s^{-1} for the tangential velocity of an object with a distance of 10 kpc. Moreover, proper motions should be linked to an inertial reference system and this correction itself might have larger uncertainties that could result in errors worse than ± 1 mas/yr.

To avoid such errors from the corrections, Brosche et al. (1983) have determined the proper motions of

Send offprint requests to: L. Chen, e-mail: chenlic@online.sh.cn

reference stars in the fields of globular clusters relative to a large number of extragalactic objects, using the Lick plates taken for the NPM program. They so reduced the data directly to an inertial system. Using the above method, Brosche et al. (1985) obtained absolute proper motions of 42 stars in the globular cluster NGC 4147 and found the mean absolute proper motion of $\mu_\alpha \cos\delta = -2.7 \pm 0.6$ mas/yr, $\mu_\delta = +0.9 \pm 0.6$ mas/yr (in 1991, they recalculated the both errors as ± 1.3 mas/yr). One problem in their work is, that the number of observed stars is too small and no photometric data are given. Since also the proper motion accuracy of individual stars is poor, membership cannot be estimated reliably and only three field stars in the sample were found. Another problem is that Brosche et al. (1985) used the AGK3 Catalogue to determine the positions of reference stars so that their results still unavoidably contain systematic differences from an inertial system. Now we can fortunately use the Hipparcos Catalogue, which is the best optical realization of the International Celestial Reference System, to minimize such a difference.

The colour-magnitude diagram of the globular cluster NGC 4147 was given earlier by Sandage & Walker (1955) and was studied by Friel et al. (1987) later. Aurière & Lauzeral (1991) presented the BV CCD photometry of this cluster and presented a CMD of 532 stars up to $V = 21$ within a $100'' \times 160''$ area. In the CMD, they found a red giant $25''$ away from the cluster center, which was about 1 mag brighter and 0.4 mag redder than other red giants in the cluster. The giant is located on the extension of the red giant branch (RGB) of the cluster CMD but it may also be a field star. The proper motion data of this star may provide a clarification of its membership.

In the present work more accurate absolute proper motions for more stars in the cluster NGC 4147 region are determined. With the proper motion result, the membership probabilities of the stars are estimated using the maximum likelihood method. Meanwhile, multi-colour photometry was made of stars in the cluster. The proper motion membership probability is used to purify the CMDs. Then, with this member sample, a more reliable mean absolute proper motion of the cluster is deduced.

2. Observations and photometric reduction

Three first epoch plates were taken with the 40 cm refractor ($f = 6895$ mm) at Sheshan station of Shanghai Astronomical Observatory in 1958 (see Table 1). All of these were taken without filter but are roughly in the B-passband. Perhaps due to weather changes during the observations, the number of detectable stars on the plates varies significantly, although the exposure times of these plates are not very different. Altogether, there are 115 different stars measured on the three plates.

All plates were scanned using the PDS-1010MS instrument of Purple Mountain Observatory, Chinese Academy of Sciences. Window scanning was used, with the initial coordinates converted from the CCD data (see below). The second epoch data in this paper are CCD frames taken in 1996 with 2.34 m Vainu Bappu telescope at Kavalur, India (focal length 7558 mm, geographic position: E121°11′11.3″, N31°05′47.6″, altitude 713 m). Table 2 gives the detailed observing information. The main purpose of taking these frames is to do $BVRI$ photometry, but they are also of interest for astrometry. Of these, four B-passband frames were used for the proper motion determination. The CCD was made by Photometrics Inc., type TK1024AB2, 1024×1024 pixels, each $24\mu \times 24\mu$, the field is $11' \times 11'$. This field size defines the investigated region in our work. Image processing of the CCD data frames was done in the usual manner using bias subtraction and flat-fielding. The coincidence of the flat field frames (summed for each colour band) is better than a few percent in all the filters. The magnitudes were determined using DAOPHOT2 and ALLSTAR2 profile fitting softwares (Stetson 1987, 1992). The stellar point spread function (PSF) was evaluated using the Penny model of DAOPHOT2 from several uncontaminated stars present in each frame. The image parameters and errors

Table 1. The three first-epoch plates taken with 40 cm refractor at sheshan station of Shanghai Observatory

Plate No.	Observation date	Exposure	No. Stars
CL 58001	$1958-03-29$	$60^{\rm m}$	38
CL 58003	$1958-02-13$	$45^{\rm m}$	24
CL 58004	$1958-02-13$	$60^{\rm m}$	112

Table 2. CCD Observational material taken with the Vainu Bappu Telescope

Frame	Observation date	Passband	Exposure (s)
24m4147i27f	$1996-03-24$	I	60
24m4147i28f	$1996-03-24$	I	180
24m4147i29f	$1996-03-24$	I	900
24m4147r30f	$1996-03-24$	R	60
24m4147r31f	$1996-03-24$	R	180
24m4147r32f	$1996-03-24$	R	900
24m4147b33f	$1996-03-24$	B	180
24m4147b34f	$1996-03-24$	B	300
24m4147b35f	$1996-03-24$	B	1800
24m4147v36f	$1996-03-24$	V	60
24m4147v37f	$1996-03-24$	V	180
24m4147v38f	$1996-03-24$	V	1200
24m4147b30f	$1996-03-25$	B	1800
24m4147v31f	$1996-03-25$	V	1200
24m4147r32f	$1996-03-25$	R	900
24m4147i33f	$1996-03-25$	I	900

Table 3. Coefficients of linear transformation of 3 B-passband CCD frames to the standard CCD frame (24m4147b33f)

Frame	X coordinate			Y coordinate		
	a	b	c	a'	b'	c'
24m4147b34f	1.00	0.00	0.38	0.00	1.00	0.82
24m4147b35f	1.00	0.00	−0.31	0.00	1.00	1.49
24m4147b30f	1.00	0.00	16.42	0.00	1.00	−21.80

Note: $x' = ax + by + c, y' = a'x + b'y + c'$, in units of pixel.

Table 4. Average positional accuracy of the position of one star on the B-passband CCD frames (unit: pixel)

Frame	σ_x	σ_y	star number
24m4147b33f	0.22	0.20	106
24m4147b34f	0.18	0.17	103
24m4147b35f	0.20	0.19	104
24m4147b30f	0.21	0.16	101

provided by DAOPHOT2 and ALLSTAR2 were used to reject poor measurements. About 10% of the stars were rejected in this process. After all the frames were reduced, Stetson's (1992) DAOMATCH and DAOMASTER routines were used to cross identify the stars measured on different frames of the cluster region.

In order to estimate the astrometric accuracy of the four B-passband CCD frames, we took the first frame (24m4147b33f) as a standard frame. Rectangular stellar positions (in units of pixel) in the other three B-passband frames were linearly transformed to the same system as the standard frame (coefficients of the transformation are listed in Table 3). The few stellar positions in those three frames that have significant coordinate deviations (exceeding 2 pixels) in comparison with the standard frame (probably due to erroneous identification or severe image blending) were rejected before further reductions. Then we obtained an average frame in which each stellar position is the mean of the (x, y) coordinate in the four frames (in the same system). Coordinate deviations for stars in all four frames with respect to the average frame were calculated and stars with x or y deviations larger than 0.7 pixel were rejected. The resulting (x, y) coordinate dispersion for the remaining stars is about 0.2 pixel, corresponding to $0''.13$ (see Table 4). We only used the remaining stars for further astrometric reductions (Table 4 also lists the number of stars used in each frame).

The CCD instrumental magnitudes have been calibrated using local standards in the cluster field by Christian et al. (1985). The equations relating the instrumental magnitudes to standard magnitudes are:

$$B = b - (0.3213 \pm 0.0165)(b - v),$$
$$V = v - (0.1528 \pm 0.0118)(v - i),$$

Table 5. Photometric errors (output of DAOPHOT) from the fit to the star profile

Parameter	Median error	Maximum error
V	0.025	0.296
$B - V$	0.043	0.404
$V - R$	0.045	0.301
$V - I$	0.043	0.303

$$R = r + (0.0738 \pm 0.0287)(v - r),$$
$$I = i + (0.0706 \pm 0.0156)(v - i),$$

where b, v, r, i represent instrumental magnitudes while B, V, R, I represent standard magnitudes.

The limiting magnitude of the photometry is close to $V = 22$ mag, in this paper however, only stars with proper motion data available were considered, whose limiting magnitude is about $B = 17.6$. Table 5 shows the photometric error distribution for the 115 stars. The complete photometric work will be given in a separate paper by A.C. Gupta.

3. Proper motion reduction and membership probability estimation

For the reduction of the proper motions we used the catalogue of positions and proper motions of 82 stars based on Hipparcos system given by Geffert et al. (1997) reduced from positions of stars on plates taken with the 30 cm refractor ($f = 5130$ mm) over 60 years (Brosche et al. 1985). The catalogue is in the J2000 system with an epoch of 1950. It has 54 stars in common with the present work. These stars served as reference stars. A Central overlapping procedure (Russell 1976; Wang et al. 1996) was used for the proper motion reduction. The four B passband second epoch CCD frames were treated in the same way as the three first epoch plates and all will be designated as "plates" hereafter. The x, y coordinates of the stellar images in the plates with units of CCD pixel were multiplied by a suitable factor in order to convert them into numbers in units of mm, which are close to the units of the measurements of the first epoch plates. All of the 54 reference stars were adjusted in each iteration of position and proper motion reduction.

In the reduction we checked the need for different plate constants. It is shown that six plate constants would be enough for our central overlap procedure. Thus, higher order polynomials of the positions and additional magnitude and color terms were not necessary. Figure 1 gives the residuals in x and y with respect to magnitude and color, respectively, for plate CL 58004 (here we selected only stars which were seen on at least two of the first epoch plates), Fig. 2 gives the same relations for CCD

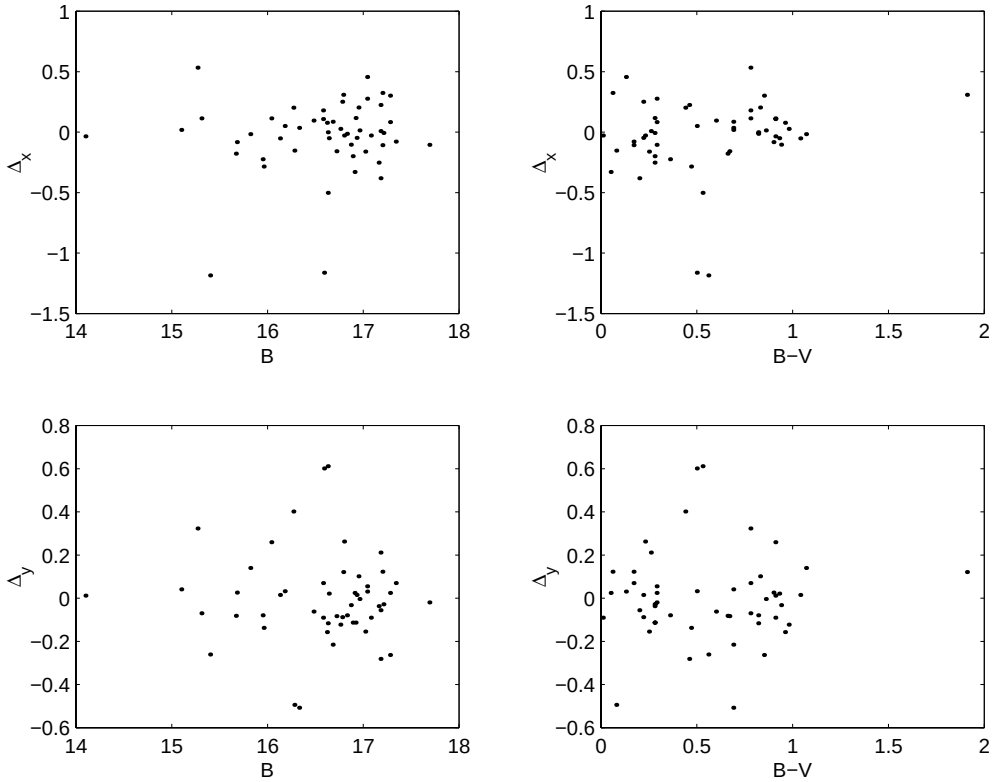

Fig. 1. Plate CL 58004: residuals in X and Y vs. mag and color

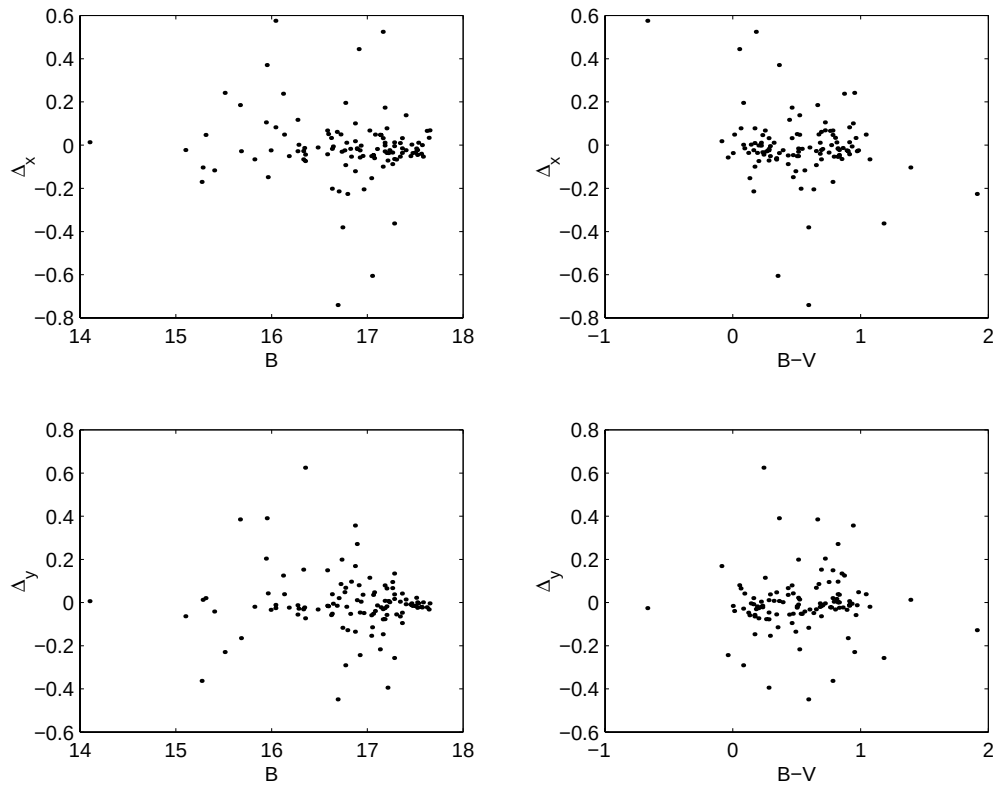

Fig. 2. CCD frame: residuals in X and Y vs. mag and color

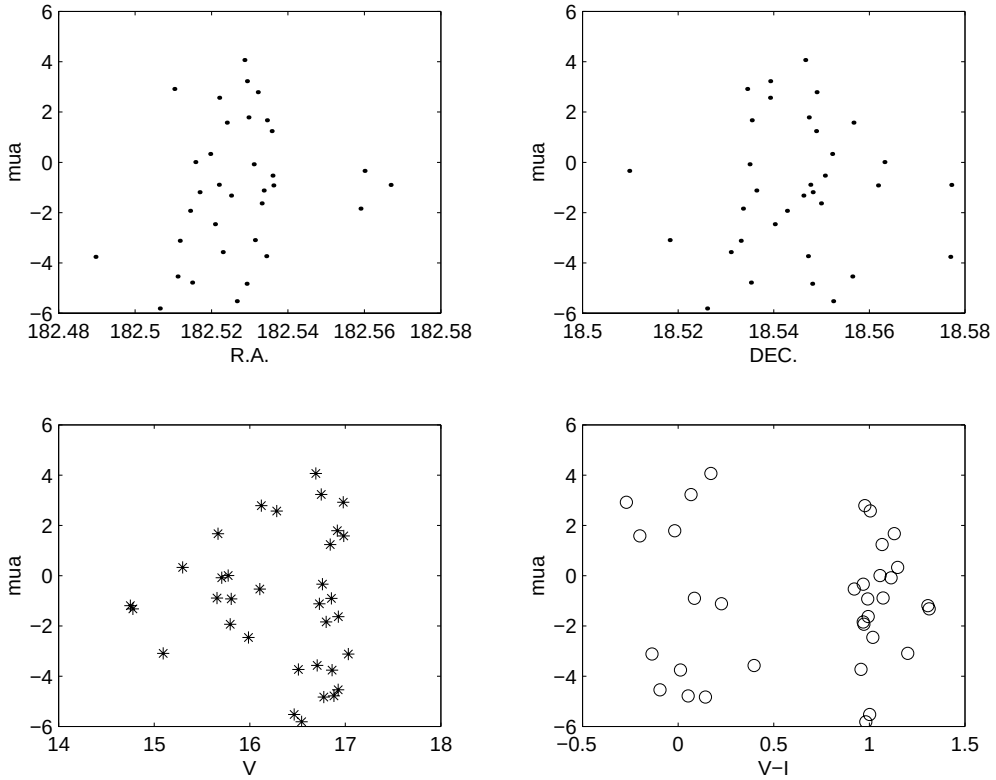

Fig. 3. $\mu_\alpha \cos\delta$ vs. RA, DEC., mag and color

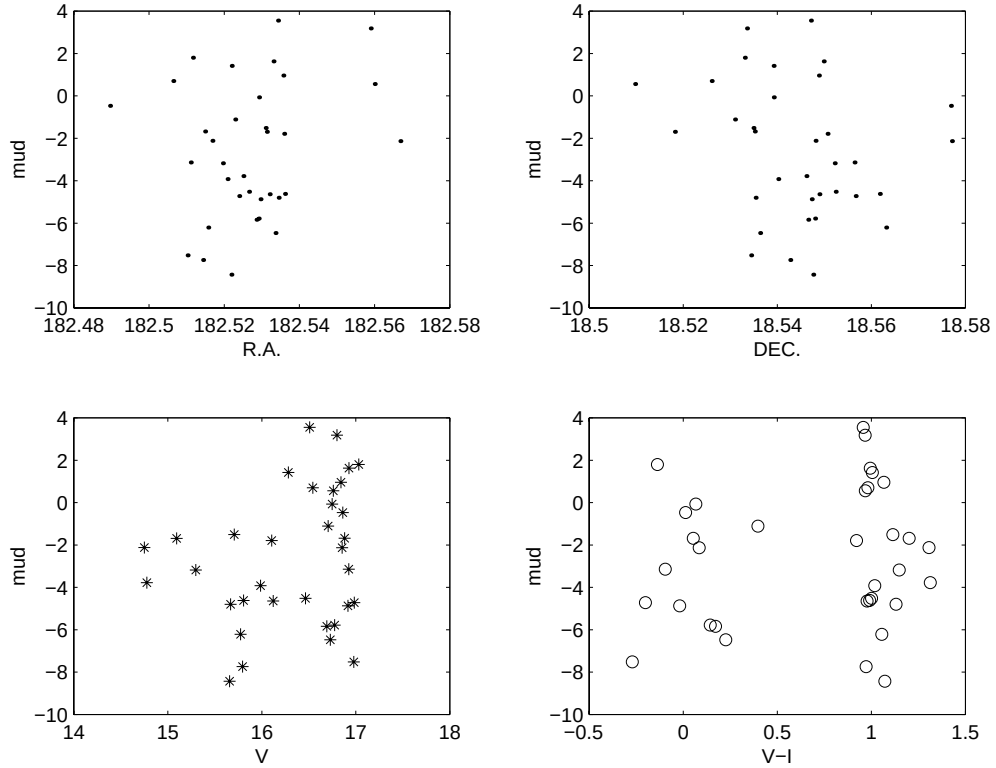

Fig. 4. μ_δ vs. RA, DEC., mag and color

Table 6. Internal astrometric errors

Parameter	Median error	Maximum error
α	$0^{s}.0041$	$0^{s}.0394$
δ	$0''.059$	$0''.404$
$\mu_\alpha \cos\delta$	1.45 mas/yr	15.13 mas/yr
μ_δ	1.39 mas/yr	11.88 mas/yr

frame 25m4147b30f. Both figures show no significant systematic trend. From these two figures one can find that the positional accuracy of the CCD frames is about $0''.13$, which is consistent with our estimation above, while the positional accuracy for photographic plates is about $0''.20$ (after rejecting several stars with large deviations).

After the fourth iteration positions and proper motions from two subsequent iteration steps showed little deviations. Mean differences in position were smaller than $0''.03$, the rms is smaller than 6 mas and the differences in proper motion were below 1 mas/yr, the rms below 0.15 mas/yr. We took the positions and proper motions of 115 stars given by this iteration as the final outcome and their errors are listed in Table 6. It should be pointed out that the errors given in Table 6 are only estimates of internal errors in the adjustment process and are undoubtedly underestimated to some extent. In our following discussion on the membership probabilities, we shall give more realistic error estimates.

To search for possible systematic errors in our resulting proper motions, we selected a test sample of 34 stars with membership probabilities greater than 0.7 and of horizontal branch or the giant branch nature from the V versus $(V-I)$ diagram (see Fig. 6 and text below). From this sample, the resulting proper motions were plotted against R.A., DEC., V and $V-I$, respectively, as is shown in Fig. 3 and Fig. 4. No apparent systematic dependence could be found in these figures. However, as is seen in these figures, the proper motion dispersions are much greater than the internal errors in Table 6. The proper motion dispersions here are 2.7 mas/yr in right ascension and 3.2 mas/yr in declination, respectively, which should be related to the astrometric accuracy of the CCD frames and the photographic plates. For those stars which are seen on all three plates and four CCD frames, the accuracy is rather 3 mas/yr.

For the membership probability estimation, we used a maximum likelihood method with a 9-parameter Gaussian model as follows:

$$\begin{aligned}\Phi(\mu_{xi},\mu_{yi}) &= \Phi_{\rm c}(\mu_{xi},\mu_{yi})+\Phi_{\rm f}(\mu_{xi},\mu_{yi}),\\ \Phi_{\rm c}(\mu_{xi},\mu_{yi}) &= \frac{n_{\rm c}}{2\pi(\sigma_0^2+\varepsilon_{xi}^2)^{1/2}(\sigma_0^2+\varepsilon_{yi}^2)^{1/2}}\\ &\quad\cdot\exp\left\{-\frac{1}{2}\left[\frac{(\mu_{xi}-\mu_{x_{\rm c}})^2}{\sigma_0^2+\varepsilon_{xi}^2}+\frac{(\mu_{yi}-\mu_{y_{\rm c}})^2}{\sigma_0^2+\varepsilon_{yi}^2}\right]\right\},\end{aligned}$$

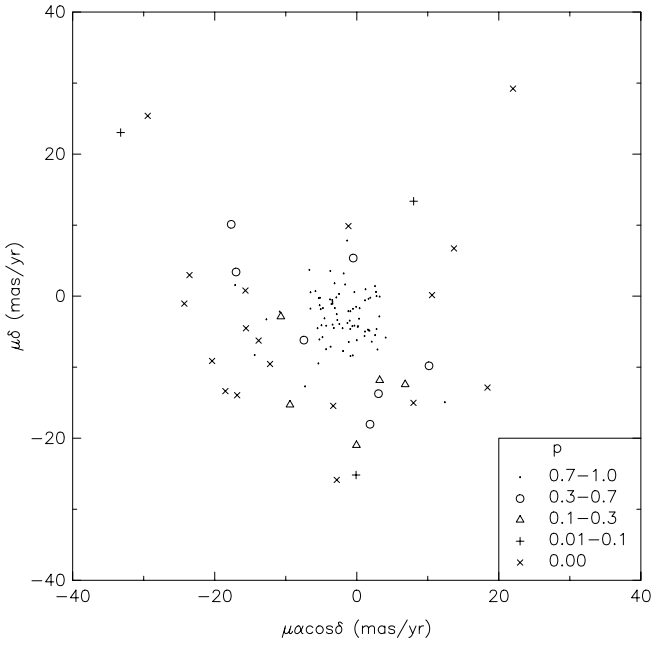

Fig. 5. Vector point diagram of proper motions

$$\begin{aligned}\Phi_{\rm f}(\mu_{xi},\mu_{yi}) &= \frac{1-n_{\rm c}}{2\pi(1-\rho^2)^{1/2}(\sigma_{x0}^2+\varepsilon_{xi}^2)^{1/2}(\sigma_{y0}^2+\varepsilon_{yi}^2)^{1/2}}\\ &\quad\cdot\exp\left\{-\frac{1}{2(1-\rho^2)}\left[\frac{(\mu_{xi}-\mu_{x\rm f})^2}{\sigma_{x0}^2+\varepsilon_{xi}^2}\right.\right.\\ &\quad-\frac{2\rho(\mu_{xi}-\mu_{x\rm f})(\mu_{yi}-\mu_{y\rm f})}{(\sigma_{x0}^2+\varepsilon_{xi}^2)^{1/2}(\sigma_{y0}^2+\varepsilon_{yi}^2)^{1/2}}\\ &\quad\left.\left.+\frac{(\mu_{yi}-\mu_{yf})^2}{\sigma_{y0}^2+\varepsilon_{yi}^2}\right]\right\}.\end{aligned}$$

where (μ_{xi},μ_{yi}) and $(\varepsilon_{xi},\varepsilon_{yi})$ are the proper motion components of the i-th star and their observing errors, respectively. The centers of the cluster and of the field stars in the proper motion vector point diagram, $(\mu_{x\rm c},\mu_{y\rm c})$ and $(\mu_{x\rm f},\mu_{y\rm f})$, the intrinsic dispersions of the proper motions of the cluster members and field stars σ_0 and $(\sigma_{x0},\sigma_{y0})$, the correlation coefficient ρ, and $n_{\rm c}$, the fraction of all member stars, have to be determined in the fit. The 9 parameters were determined by the maximum likelihood procedure and their uncertainties by the second derivative of the likelihood function. The results are summarized in Table 7. Once these parameters are determined, the membership probability of i-th star is given by

$$p_i=\Phi_{\rm c}(\mu_{xi},\mu_{yi})/\Phi(\mu_{xi},\mu_{yi}).$$

Figure 5 gives the vector point plot diagram of the 115 stars, with different symbols for different probabilities. The number of stars with different membership probabilities is shown in Table 8. According to the value of $n_{\rm c}$ in Table 7, there should be 70 cluster stars, under the assumption that stars with $p\le 0.6$ can be regarded as field stars.

Table 7. Estimates of model parameters from maximum likelihood fitting

Parameter	Estimate
μ_{xc}	-1.65 ± 0.39 mas/yr
μ_{yc}	-2.69 ± 0.38 mas/yr
μ_{xf}	-5.30 ± 0.66 mas/yr
μ_{yf}	-4.13 ± 2.63 mas/yr
$\sigma_{\rm o}$	2.58 ± 0.33 mas/yr
$\sigma_{x_{\rm o}}$	12.69 ± 0.10 mas/yr
$\sigma_{y_{\rm o}}$	11.52 ± 1.40 mas/yr
ρ	-0.105 ± 0.095
$n_{\rm c}$	0.698 ± 0.051

Table 8. Membership probability distribution of stars in the region of NGC 4147

Prob.	Number of stars
1.00−0.90	59
0.90−0.80	16
0.80−0.70	6
0.70−0.60	2
0.60−0.50	2
0.50−0.40	2
0.40−0.30	1
0.30−0.20	2
0.20−0.10	3
0.10−0.01	3
0.00	19

The values in Table 7 provide a possibility of estimating the external accuracy of the proper motion results in this work. Since NGC 4147 is very far away from us the contribution by the internal motions of the cluster stars can be neglected and σ_0 can be regarded entirely as the observational dispersion. The dispersion of 2.6 mas/yr is in good agreement with the error estimated from the astrometric accuracy of the CCD frames and the plates.

4. Color-magnitude diagram

The color-magnitude diagrams of V versus $B-V$, $V-R$ and $V-I$ are presented in Figs. 6–8, respectively, with different symbols for different membership probabilities as used in Fig. 5.

The characteristic behaviour of these diagrams is, on the whole, similar to the CMD of V versus $B-V$ from Aurière & Lauzeral (1991), however with a large dispersion for the cluster members, especially there are quite a few stars with large membership probabilities located above the horizontal branch. From our CMDs of V versus $V-R$ and $V-I$, it seems that there exists a second horizontal branch (somewhat similar to the second main sequence in CMD of some open clusters). It might be caused by double stars. On the other hand in our sample, we have not identified the RR Lyrae stars which would drift off the horizontal branch. Moreover, crowding problems near the cluster center caused the reduced accuracy of the photometric data, and this could be another reason for the large dispersion in the member star sequence. In our sample 54 stars, which appeared only on one of the first-epoch plates (CL 58004) and not in the catalogue of Geffert et al. (1997), have relatively large uncertainties in the membership probabilities since their proper motion estimates can only be regarded as preliminary. In addition, some of our stars with large membership probabilities have large internal proper motion errors (which can be seen in the vector point diagram of proper motions). In this case, it is likely that one or two non-members were estimated

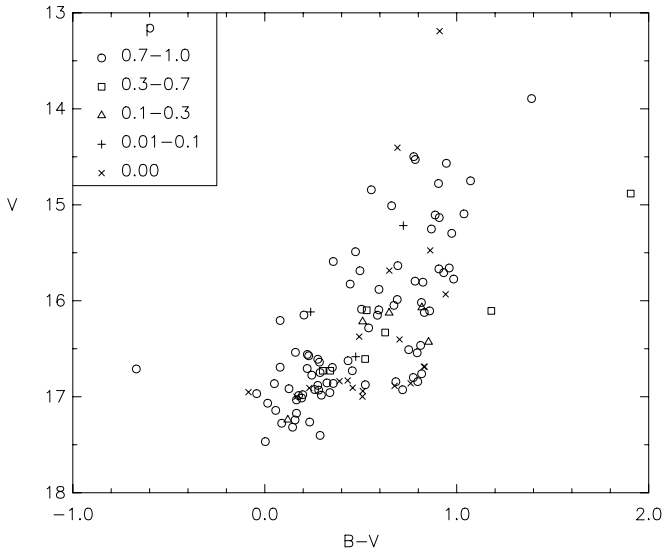

Fig. 6. Diagram of V vs. $B-V$

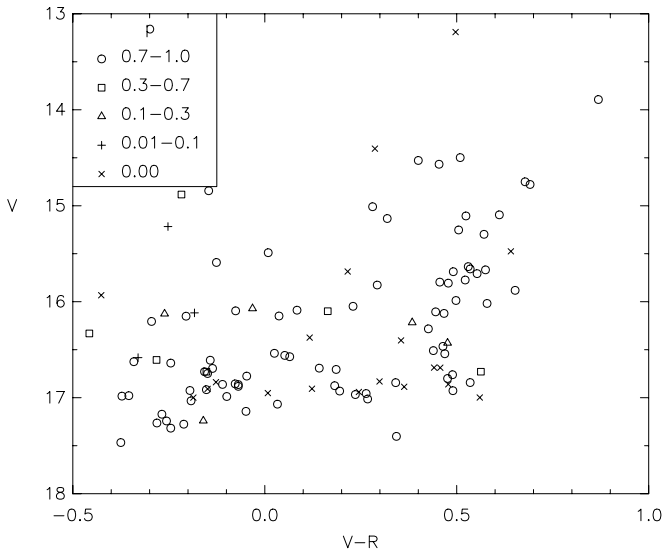

Fig. 7. Diagram of V vs. $V-R$

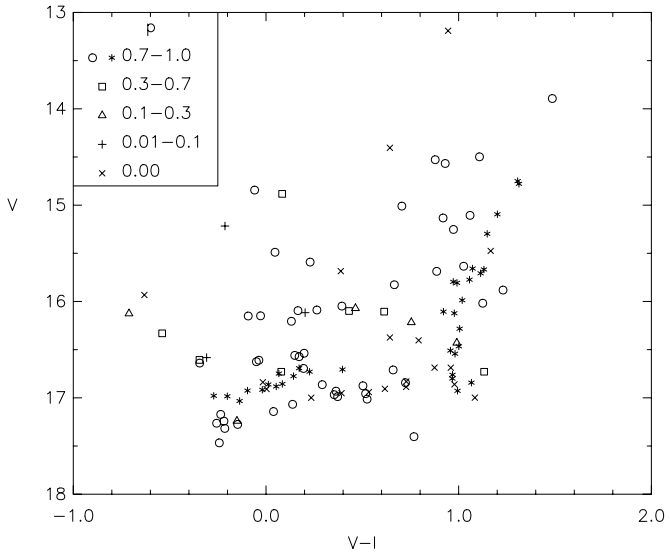

Fig. 8. Diagram of V vs. $V-I$, *: stars located on HB or GB and constitute a test sample

as member stars, which could also lead to an increase of the dispersion in the CMDs. It is interesting to note that the star sorted out by Aurière & Lauzeral (1991), being brighter than the red giants by about 1 mag and redder by 0.4 mag is, according to our result, a cluster member with a membership probability of 0.97. It is located on the extension of the red giant branch in all three CMDs. Based on this, it is very probably an AGB star which is entering or has entered already the thermal pulsation stage. Since the cluster radial velocity is large, and the star not exceedingly faint, a future radial velocity measurement may check its membership.

5. Illustration of the catalogue

In Table 9 we give absolute proper motions as well as $BVRI$ photometric data for 115 stars in the region of globular cluster NGC 4147. The investigated region is about $11' \times 11'$ in size. The limiting magnitude of 115 stars which have proper motion data available is close to $B = 17.6$ mag. The complete photometry on NGC 4147 will be given in a separate paper by A.C. Gupta. Detailed description about the observation, plate measurements and astrometric reduction can be found in Sect. 2 and Sect. 3 of this paper. In Table 9 the 115 stars were arranged in two parts. The first part includes 61 stars which appear on at least two of the first-epoch plates, or which have the position and proper motion data from Geffert et al. (1997) though it might appear on only one of their first-epoch plates. The second part includes 54 stars which appear on only one of our first-epoch plates, and these proper motions should be regarded as preliminary. The meaning of each column in Table 9 is as follows:

(1). sequence number of stars in this catalogue,
(2). sequence number in the complete photometric catalogue of A.C. Gupta,
(3). sequence number in Geffert et al. (1997),
(4). internal star ID number in Geffert et al. (1997),
(5). V magnitude,
(6). standard error of the V magnitude (in units of 0.001 mag),
(7). $B-V$ color index,
(8). standard error of $B-V$ (in units of 0.001 mag),
(9). $V-R$ color index,
(10). standard error of the $V-R$ (in units of 0.001 mag),
(11). $V-I$ color index,
(12). standard error of $V-I$ (in units of 0.001 mag),
(13). right ascension relative to J2000.0 equator and vernal equinox for epoch 2000,
(14). standard error of the right ascension (in units of 0.00001 s),
(15). declination relative to J2000.0 equator and vernal equinox for epoch 2000,
(16). standard error of the declination (in units of $0''.0001$),
(17). absolute proper motion in right ascension (in units of 0.01 mas/yr),
(18). standard error of the absolute proper motion in right ascension (in units of 0.01 mas/yr),
(19). absolute proper motion in declination (in units of 0.01 mas/yr),
(20). standard error of the absolute proper motion in declination (in units of 0.01 mas/yr),
(21). number of plates contain this star,
(22). membership probability,
(23). member selection (0: non-member, 1: member).

6. Proper motion, space velocity and orbital parameters of the cluster

We have obtained three values for absolute proper motion of the cluster, from (1) the maximum likelihood fitting $(-1.65 \pm 0.39, -2.69 \pm 0.38)$ mas/yr; (2) the mean value of proper motions of all stars, weighted by membership probabilities $(-2.08 \pm 0.41, -3.07 \pm 0.39)$ mas/yr; (3) the mean value of proper motions of all members, equally weighted $(-1.94 \pm 0.47, -2.86 \pm 0.39)$ mas/yr. In comparison, Geffert et al. (1997) gave the value $(-1.0, -3.5)$ mas/yr (this value is also used by Odenkirchen et al. 1997). All these results can be regarded as consistent within the uncertainties. We take the second set as our final estimation of the absolute proper motion of the cluster. Taking into account a systematic error of the Hipparcos proper motions of ± 0.25 mas/yr, we have the absolute proper motion of the cluster as $(-2.08 \pm 0.48, -3.07 \pm 0.46)$ mas/yr. We calculated the space velocity of NGC 4147 in a system of galactic standard of rest using a distance of the Sun from the galactic center of 8 kpc, a rotation of 225 km s^{-1} at the place of the Sun,

Table 9. Absolute proper motions and $BVRI$ photometry of 115 stars in the region of globular cluster NGC 4147

No.	N(Gu)	N(Ge)	I(Ge)	V	σ_V	$B-V$	$\sigma_{(B-V)}$	$V-R$	$\sigma_{(V-R)}$	$V-I$	$\sigma_{(V-I)}$	R.A.(J2000.0)	σ_α	DEC(J2000.0)	σ_δ	$\mu_\alpha \cos\delta$	$\sigma_{\rm PA}$	μ_δ	$\sigma_{\rm PD}$	N	P	Mem.
(1)	(2)	(3)	(4)	(5)	(6)	(7)	(8)	(9)	(10)	(11)	(12)	(13)	(14)	(15)	(16)	(17)	(18)	(19)	(20)	(21)	(22)	(23)
1	162	13	2004	14.405	1	.691	3	.287	4	.643	4	12 09 58.47542	410	+18 34 08.8710	329	−2037	124	−912	77	3	.00	0
2	274	14	2020	16.429	7	.853	7	.476	8	.990	8	12 10 01.65558	743	+18 32 40.0010	885	322	228	−1184	176	1	.18	0
3	285	15	3020	17.172	14	.165	14	−.268	17	−.235	46	12 10 01.81731	171	+18 32 07.3822	357	−100	49	−346	74	1	.98	1
4	316	16	2019	17.067	107	.015	107	.033	107	.138	108	12 10 02.32240	245	+18 32 51.4810	531	−652	72	−176	113	1	.89	1
5	327	17	3019	16.979	35	.198	48	−.354	45	−.271	39	12 10 02.46625	891	+18 32 04.0494	288	292	270	−752	61	1	.78	1
6	347	18	2015	16.925	13	.260	14	−.195	23	−.096	19	12 10 02.67214	85	+18 33 23.1216	934	−454	24	−314	190	1	.95	1
7	357	19	3014	17.032	27	.165	29	−.192	35	−.137	32	12 10 02.80345	443	+18 31 59.0971	926	−312	130	180	191	1	.93	1
8	403	20	3015	15.796	12	.783	16	.456	14	.972	13	12 10 03.45550	773	+18 32 33.8945	1309	−193	239	−774	294	3	.92	1
9	407	21	3018	16.018	18	.816	23	.579	21	1.125	19	12 10 03.54818	187	+18 32 21.0436	1352	258	56	−550	288	3	.89	1
10	414	22	3017	16.881	8	.276	18	−.069	19	.053	14	12 10 03.58597	632	+18 32 06.8464	390	−478	194	−168	85	1	.96	1
11	433	23	2010	15.774	1	.984	4	.522	2	1.056	2	12 10 03.78321	91	+18 33 47.3631	443	1	28	−621	88	2	.94	1
12	455	24	2030	14.750	4	1.072	8	.678	4	1.306	7	12 10 04.05190	187	+18 32 53.2787	604	−119	60	−212	137	3	.98	1
13	518	25	2014	15.298	3	.974	7	.571	3	1.148	4	12 10 04.72246	481	+18 33 07.9647	353	33	148	−318	80	2	.97	1
14	537	26	102	17.403	111	.288	125	.343	112	.768	112	12 10 04.93443	537	+18 32 04.3378	263	−322	159	−450	53	1	.97	1
15	553	28	3034	15.987	85	.690	116	.498	89	1.018	85	12 10 05.01653	779	+18 32 24.7068	1404	−246	239	−392	291	1	.96	1
16	572	29	2035	15.658	8	.961	17	.535	8	1.072	17	12 10 05.26129	461	+18 32 51.4847	931	−89	139	−843	202	2	.88	1
17	586	30	2044	15.106	6	.888	46	.524	20	1.059	27	12 10 05.38257	158	+18 32 34.8306	542	−342	50	−106	112	3	.97	1
18	594	31	2036	16.639	17	.285	57	−.245	179	−.344	174	12 10 05.41651	441	+18 32 56.2000	487	−517	131	−24	95	2	.93	1
19	599	32	111	16.705	4	.221	39	.186	7	.397	16	12 10 05.50434	411	+18 31 51.6532	225	−357	127	−111	43	1	.97	1
20	604	33	200	15.634	93	.693	114	.530	93	1.026	100	12 10 05.52983	499	+18 32 22.9200	4036	−135	145	781	868	1	.92	1
21	616	34	202	13.894	6	1.390	7	.869	12	1.486	203	12 10 05.60585	267	+18 32 11.5594	606	41	83	−171	133	3	.97	1
22	620	35	211	15.591	35	.357	240	−.126	50	.229	39	12 10 05.61201	841	+18 32 45.1903	970	−288	242	−19	199	2	.96	1
23	632	36	2013	16.983	20	.295	26	−.372	79	−.201	28	12 10 05.75801	211	+18 33 24.0603	214	158	63	−472	44	1	.95	1

Table 9. continued

No.	N(Gu)	N(Ge)	I(Ge)	V	σ_V	$B-V$	$\sigma_{(B-V)}$	$V-R$	$\sigma_{(V-R)}$	$V-I$	$\sigma_{(V-I)}$	R.A.(J2000.0)	σ_α	DEC(J2000.0)	σ_δ	$\mu_\alpha \cos\delta$	$\sigma_{\rm PA}$	μ_δ	$\sigma_{\rm PD}$	N	P	Mem.
(1)	(2)	(3)	(4)	(5)	(6)	(7)	(8)	(9)	(10)	(11)	(12)	(13)	(14)	(15)	(16)	(17)	(18)	(19)	(20)	(21)	(22)	(23)
24	637	37	20441	15.489	46	.473	100	.009	72	.047	165	12 10 05.80417	1444	+18 32 35.0119	1074	−667	442	370	233	1	.74	1
25	664	38	2045	14.778	46	.905	93	.691	46	1.313	46	12 10 06.02875	903	+18 32 46.2952	683	−132	282	−378	158	3	.97	1
26	670	40	992	14.498	32	.776	75	.509	90	1.108	256	12 10 06.09253	2353	+18 32 32.7600	1632	−1273	789	−327	377	3	.83	1
27	669	39	201	15.826	104	.445	112	.293	115	.666	107	12 10 06.09790	518	+18 32 22.7916	2296	−200	152	−452	467	3	.95	1
28	685	41	994	14.568	74	.946	137	.454	94	.930	75	12 10 06.21084	1140	+18 32 30.3774	3086	−249	362	30	648	2	.92	1
29	690	42	991	15.01	30	.661	35	.281	59	.705	43	12 10 06.25147	997	+18 32 37.2600	2928	116	312	−499	656	3	.92	1
30	701	43	993	14.844	41	.555	81	−.146	54	−.059	93	12 10 06.32978	2567	+18 32 33.9937	2214	−62	750	−422	510	2	.90	1
31	702			16.205	133	.080	144	−.295	164	.132	218	12 10 06.36009	2404	+18 32 13.7097	2369	−728	942	−1271	609	3	.70	0
32	707			16.099	143	.531	165	.164	158	.431	202	12 10 06.39677	1807	+18 32 42.3934	3761	−1768	824	1011	1114	2	.50	0
33	705	44	4048	15.252	50	.868	61	.505	50	.973	50	12 10 06.41106	817	+18 32 23.3615	1221	−340	256	−402	282	2	.95	1
34	709	45	4036	16.573	27	.229	50	.065	41	.172	115	12 10 06.44942	231	+18 32 19.7087	1915	317	62	−287	411	2	.87	1
35	714	46	995	14.528	8	.784	37	.400	27	.878	32	12 10 06.53825	922	+18 32 31.8788	636	110	286	−561	139	3	.94	1
36	725			14.883	32	1.906	45	−.217	244	.084	177	12 10 06.55072	1580	+18 32 32.0647	2006	−1700	622	340	508	2	.41	0
37	713	47	1020	16.863	64	.050	189	−.069	82	.292	67	12 10 06.57521	1648	+18 33 01.7684	1640	−430	505	−417	348	3	.93	1
38	767	50	1038	16.775	4	.245	43	−.047	52	.143	46	12 10 07.00697	571	+18 32 52.9171	825	−483	175	−578	173	1	.92	1
39	769	49	4033	16.748	151	.288	159	−.149	156	.067	155	12 10 07.02543	659	+18 32 21.2611	688	323	199	−7	148	1	.91	1
40	777			16.088	37	.504	120	.084	39	.264	41	12 10 07.02915	3939	+18 32 14.7901	3628	−1713	1513	155	912	3	.75	1
41	781	51	1037	16.916	8	.126	39	−.152	32	−.019	50	12 10 07.12102	1422	+18 32 50.4311	432	179	430	−487	85	1	.94	1
42	802	52	1034	16.149	70	.204	116	.037	85	−.028	70	12 10 07.32570	264	+18 32 40.2246	781	166	75	−38	171	1	.95	1
43	803	53	105	16.537	123	.160	130	.025	142	.198	202	12 10 07.33760	922	+18 32 34.9067	1055	−497	287	−411	231	2	.94	1
44	813			15.707	10	.932	28	.553	12	1.114	10	12 10 07.45075	115	+18 32 05.7215	110	−8	46	−151	28	3	.98	1
45	821	54	210	15.133	72	.909	112	.319	74	.919	75	12 10 07.51455	910	+18 32 31.7557	2198	−431	295	−748	503	3	.90	1
46	819	55	4013	15.095	1	1.038	29	.611	4	1.201	3	12 10 07.52803	531	+18 31 05.5965	537	−309	172	−169	118	3	.97	1

Table 9. continued

No.	N(Gu)	N(Ge)	I(Ge)	V	σ_V	$B-V$	σ_{B-V}	V-R	σ_{V-R}	V-I	σ_{V-I}	R.A.(J2000.0)	σ_α	DEC(J2000.0)	σ_δ	$\mu_\alpha \cos\delta$	$\sigma_{\rm PA}$	μ_δ	$\sigma_{\rm PD}$	N	P	Mem.
(1)	(2)	(3)	(4)	(5)	(6)	(7)	(8)	(9)	(10)	(11)	(12)	(13)	(14)	(15)	(16)	(17)	(18)	(19)	(20)	(21)	(22)	(23)
47	825	56	10000	16.048	16	.673	24	.230	89	.394	116	12 10 07.56862	549	+18 32 15.3593	478	−507	168	−184	99	2	.95	1
48	830			15.932	296	.942	328	−.426	301	−.631	303	12 10 07.60588	658	+18 32 33.6152	1922	2200	285	2921	553	2	.00	0
49	836	57	1023	16.122	4	.831	29	.467	10	.977	4	12 10 07.70352	510	+18 32 56.2755	575	279	147	−464	119	1	.92	1
50	861	59	4026	16.729	20	.456	41	−.157	45	.226	41	12 10 08.07265	927	+18 32 10.8512	1357	−112	283	−647	298	1	.94	1
51	885	60	4022	15.668	9	.907	13	.575	9	1.131	12	12 10 08.27772	653	+18 32 07.4741	335	167	210	−480	74	3	.95	1
52	889	61	4017	17.142	100	.057	100	−.049	100	.039	101	12 10 08.37028	702	+18 31 47.8092	615	−33	200	−416	129	1	.97	1
53	895	62	1031	15.881	162	.595	168	.652	162	1.230	162	12 10 08.41655	297	+18 32 44.7085	617	14	96	−433	125	2	.97	1
54	900			16.559	19	.222	29	.052	20	.149	82	12 10 08.48082	877	+18 32 59.8255	571	−367	400	−712	169	3	.88	1
55	911	63	1027	16.105	7	.859	68	.445	8	.921	8	12 10 08.62942	263	+18 33 02.4766	643	−53	71	−179	133	1	.98	1
56	917	64	1017	15.806	4	.824	7	.478	4	.991	4	12 10 08.67930	85	+18 33 42.5123	588	−92	26	−462	132	2	.97	1
57	1022	65	4015	16.609	3	.276	3	−.142	4	−.037	10	12 10 09.99845	332	+18 31 48.7952	852	−282	92	−255	181	2	.97	1
58	1188	67	1005	13.191	2	.911	2	.497	4	.945	21	12 10 12.62842	92	+18 34 36.2468	116	−2428	28	−105	28	3	.00	0
59	1309	69	31	15.687	35	.496	43	.491	35	.886	35	12 10 17.84725	243	+18 27 59.6205	381	−534	79	−29	81	2	.93	1
60	1346	70	32	15.475	10	.862	13	.641	12	1.166	12	12 10 20.82795	417	+18 29 13.8209	414	−1849	133	−1337	83	2	.00	0
61	1360	71	33	16.930	8	.281	90	.195	13	.363	9	12 10 21.94267	387	+18 35 01.6099	1279	−56	112	−836	262	1	.91	1
62	64			16.686	3	.833	4	.441	8	.875	34	12 09 52.84501	152	+18 33 28.6193	229	−1567	81	79	75	1	.00	0
63	146			16.861	2	.357	13	−.110	9	.012	4	12 09 57.51922	106	+18 34 36.9714	168	−376	56	−47	55	1	.96	1
64	247			16.687	1	.829	4	.457	2	.959	4	12 10 00.87939	69	+18 33 14.2702	133	−1684	37	−1395	44	1	.00	0
65	258			16.886	28	.676	28	.363	29	.727	28	12 10 01.23428	144	+18 30 22.7357	184	1841	77	−1287	60	1	.00	0
66	271			16.542	4	.794	6	.469	14	.981	12	12 10 01.55697	165	+18 31 33.8247	171	−581	84	70	52	1	.87	1
67	279			16.875	2	.524	18	.182	6	.503	8	12 10 01.73706	1176	+18 32 00.2506	100	−345	593	−54	32	1	.94	1
68	293			16.860	17	.760	23	.478	17	.978	18	12 10 01.97877	786	+18 32 04.6451	249	798	421	−1502	82	1	.00	0
69	378			16.838	16	.389	25	−.127	29	−.016	46	12 10 02.94869	56	+18 36 39.7749	34	−1221	30	−955	11	1	.00	0

Table 9. continued

No.	N(Gu)	N(Ge)	I(Ge)	V	σ_V	$B-V$	σ_{B-V}	$V-R$	σ_{V-R}	$V-I$	σ_{V-I}	R.A.(J2000.0)	σ_α	DEC(J2000.0)	σ_δ	$\mu_\alpha \cos\delta$	$\sigma_{\rm PA}$	μ_δ	$\sigma_{\rm PD}$	N	P	Mem.
(1)	(2)	(3)	(4)	(5)	(6)	(7)	(8)	(9)	(10)	(11)	(12)	(13)	(14)	(15)	(16)	(17)	(18)	(19)	(20)	(21)	(22)	(23)
70	420			16.940	10	.511	14	.245	12	.534	17	12 10 03.71153	179	+18 29 39.7286	204	1369	95	673	67	1	.00	0
71	427			17.013	24	.192	39	.268	27	.525	25	12 10 03.71866	141	+18 31 48.2135	263	−274	71	−336	84	1	.98	1
72	431			16.998	112	.509	114	.560	123	1.084	135	12 10 03.76098	98	+18 32 57.6696	175	−1381	53	−625	57	1	.00	0
73	434			17.467	118	.003	125	−.375	135	−.242	136	12 10 03.82091	170	+18 32 43.7240	219	279	91	0	72	1	.91	1
74	460			16.830	39	.432	41	.299	50	.728	52	12 10 04.09282	234	+18 32 41.2009	296	−117	126	987	97	1	.00	0
75	461			16.625	14	.434	19	−.341	59	−.050	23	12 10 04.10201	167	+18 32 38.6264	276	211	89	−642	91	1	.88	1
76	489			16.987	14	.176	32	−.099	83	.372	41	12 10 04.33730	1624	+18 31 58.1781	472	−522	871	−129	156	1	.93	1
77	509			16.729	19	.341	41	−.152	37	.079	32	12 10 04.55740	356	+18 32 14.1933	390	−50	179	536	125	1	.53	0
78	573			16.217	79	.510	105	.384	105	.754	135	12 10 05.25731	298	+18 32 29.5882	1444	681	159	−1243	477	1	.14	0
79	575			16.282	45	.541	70	.426	46	1.005	82	12 10 05.28217	265	+18 32 21.1590	702	257	142	142	232	1	.89	1
80	587			16.403	2	.702	16	.355	17	.792	9	12 10 05.40234	42	+18 30 36.1543	162	−332	23	−1544	53	1	.00	0
81	600			16.330	18	.627	101	−.457	61	−.539	173	12 10 05.52076	923	+18 32 31.8735	874	1018	495	−980	289	1	.39	0
82	609			16.374	26	.492	404	.117	131	.643	172	12 10 05.54288	1569	+18 32 19.6394	2763	−4218	877	513	994	1	.00	0
83	619			16.126	14	.648	141	−.261	43	−.711	64	12 10 05.64112	1283	+18 32 27.7712	1218	−940	648	−1529	391	1	.21	0
84	634			16.071	35	.818	48	−.032	45	.464	37	12 10 05.83353	557	+18 32 41.9503	1600	−4	298	−2098	529	1	.22	0
85	642			16.999	50	.165	143	−.186	231	.235	72	12 10 05.84268	520	+18 32 22.8906	1011	−2355	262	297	325	1	.00	0
86	652			16.105	35	1.180	43	9.900	9899	.613	45	12 10 05.85813	2287	+18 32 42.5045	2432	187	1226	−1803	805	1	.62	0
87	663			16.116	261	.239	275	−.183	264	.203	284	12 10 06.02529	1537	+18 32 38.2974	3447	−3324	797	2303	1188	1	.01	0
88	667			16.906	76	.458	90	.123	130	.617	129	12 10 06.07352	130	+18 32 11.4392	461	1060	70	15	152	1	.00	0
89	679			15.685	54	.649	119	.216	57	.388	75	12 10 06.17299	374	+18 32 26.3971	176	−2943	190	2538	53	1	.00	0
90	696			16.729	43	.302	64	.563	52	1.132	75	12 10 06.34001	92	+18 32 08.2482	549	−744	42	−619	163	1	.65	0
91	703			16.967	171	−.042	195	.236	173	.354	193	12 10 06.36930	197	+18 32 49.5075	1266	−540	98	−948	404	1	.80	1
92	704			16.465	6	.812	17	.464	8	1.001	8	12 10 06.38870	146	+18 33 08.7063	194	−552	78	−452	64	1	.93	1

Table 9. continued

No.	N(Gu)	N(Ge)	I(Ge)	V	σ_V	$B-V$	σ_{B-V}	$V-R$	σ_{V-R}	$V-I$	σ_{V-I}	R.A.(J2000.0)	σ_α	DEC(J2000.0)	σ_δ	$\mu_\alpha \cos\delta$	$\sigma_{\rm PA}$	μ_δ	$\sigma_{\rm PD}$	N	P	Mem.
(1)	(2)	(3)	(4)	(5)	(6)	(7)	(8)	(9)	(10)	(11)	(12)	(13)	(14)	(15)	(16)	(17)	(18)	(19)	(20)	(21)	(22)	(23)
93	724			16.710	50	−.669	54	9.900	9899	.660	52	12 10 06.56439	1624	+18 33 01.8483	2046	−1437	871	−829	677	1	.71	1
94	722			15.217	19	.722	74	−.252	52	−.213	86	12 10 06.60926	486	+18 32 27.1633	1493	−10	248	−2517	455	1	.01	0
95	735			16.695	35	.352	89	−.136	54	.195	41	12 10 06.64182	2298	+18 33 01.9596	621	−1085	1159	−219	199	1	.90	1
96	738			16.095	14	.594	27	−.076	46	.166	41	12 10 06.66676	2662	+18 32 27.8457	3055	1240	1427	−1495	1011	1	.71	1
97	755			16.692	81	.080	133	.142	111	.172	118	12 10 06.86627	1315	+18 32 47.7047	2506	407	705	−584	829	1	.86	1
98	757			16.151	25	.587	150	−.205	138	−.092	48	12 10 06.89929	1100	+18 32 34.6856	2255	271	590	58	746	1	.89	1
99	801			16.952	43	−.085	52	.008	71	.392	158	12 10 07.27698	310	+18 32 28.2607	907	−282	156	−2587	291	1	.00	0
100	811			16.606	137	.523	167	−.282	146	−.345	143	12 10 07.42521	406	+18 32 44.5387	1181	306	218	−1372	391	1	.44	0
101	823			17.24	85	.120	87	−.160	92	−.151	93	12 10 07.55757	135	+18 33 01.1839	247	−1069	72	−288	81	1	.14	0
102	824			16.582	89	.474	120	−.330	93	−.308	131	12 10 07.57125	165	+18 32 37.0035	1667	801	89	1337	551	1	.01	0
103	854			16.927	35	.718	57	.490	37	.994	37	12 10 07.94796	222	+18 32 59.5974	93	−163	119	163	31	1	.93	1
104	879			16.908	48	.232	54	−.149	54	.003	54	12 10 08.21111	162	+18 32 59.3834	175	−1560	87	−452	58	1	.00	0
105	880			16.509	37	.750	52	.439	43	.957	43	12 10 08.23393	86	+18 32 49.7819	505	−373	46	355	167	1	.83	1
106	908			16.842	43	.797	85	.535	45	1.066	45	12 10 08.57991	447	+18 32 55.8666	489	124	239	96	161	1	.93	1
107	906			17.242	27	.158	27	−.256	27	−.218	28	12 10 08.58106	56	+18 31 17.6573	27	191	30	−22	8	1	.94	1
108	955			17.263	12	.234	16	−.281	14	−.256	48	12 10 09.12838	110	+18 32 26.4782	129	116	59	−60	42	1	.96	1
109	986			17.276	32	.088	32	−.211	32	−.147	35	12 10 09.44865	109	+18 33 40.1996	205	17	58	−424	67	1	.97	1
110	1079			16.956	2	.339	34	.264	23	.517	4	12 10 10.64424	193	+18 34 50.9295	212	−526	103	−611	70	1	.89	1
111	1237			16.800	2	.774	4	.476	2	.967	3	12 10 14.15875	30	+18 32 00.7982	97	−184	16	318	32	1	.84	1
112	1246			16.760	3	.817	17	.489	3	.968	4	12 10 14.40503	161	+18 30 35.1739	94	−34	86	56	31	1	.96	1
113	1267			17.317	4	.145	8	−.245	12	−.214	17	12 10 15.44225	28	+18 33 50.1917	82	−342	14	−81	27	1	.97	1
114	1278			16.855	2	.324	12	−.077	9	.085	9	12 10 16.04078	73	+18 34 37.6318	74	−90	36	−213	23	1	.98	1
115	1303			16.843	2	.683	4	.341	3	.724	3	12 10 17.43057	53	+18 31 59.3198	77	−651	28	53	25	1	.81	0

Table 10. Space motion and orbital parameters of NGC 4147

PM value	Π (km s^{-1})	Θ (km s^{-1})	Z (km s^{-1})	R_a (kpc)	R_p (kpc)	e	i
(2)	+70	−91	116	22.5	4.2	0.69	89°.2
(2)+1σ	+104	−58	123	22.0	2.3	0.81	84.2
(2)−1σ	+26	−124	109	23.5	6.9	0.55	91.7

a peculiar velocity of the Sun relative to LSR of $U = 10$ km s^{-1}, $V = 15$ km s^{-1} and $W = 8$ km s^{-1} (note that U points from the Sun to the galactic center, V is parallel to the galactic plane in the direction of the galactic rotation and W perpendicular to the galactic plane), a heliocentric distance of NGC 4147 of 18.32 kpc and a heliocentric radial velocity of NGC 4147 (from Harris 1996) of 183.2 km s^{-1}. The resulting space velocity of NGC 4147 is 164 ± 24 km s^{-1}. Taking the proper motion value from just the maximum likelihood fitting, we obtained the space velocity as 142 ± 12 km s^{-1}, which is, within the uncertainty range, in a good agreement with the above.

We didn't take into account the uncertainty of the heliocentric distance determination of the cluster in the above reductions. Let us assume the adopted distance of the cluster has a relative error of 10%. With this error assumption, we used two extreme distance values (that is, by adding $\pm 1\sigma$ variations to the adopted one) as input data for a similar calculation. The derived space velocity values are 183 ± 30 km s^{-1} and 149 ± 18 km s^{-1}, respectively, which are consistent with our adopted value of 164 ± 24 km s^{-1} within the uncertainty range.

Therefore we take the space velocity result derived without considering the distance uncertainty as input value in the following kinematic discussions.

The velocity components of NGC 4147 in the galactic standard of rest as well as the orbital parameters calculated using the potential model from Dauphole & Colin (1995) are listed in Table 10. In addition, we varied the cluster proper motion by $\pm$ 1 σ and re-calculated the corresponding velocity and orbital parameters, which are also listed in Table 10. The velocity components Π, Θ, Z are in a system of galactic standard of rest. Π points radially outwards from the galactic center to the cluster, Θ is in the direction of the galactic rotation, Z is perpendicular to the galactic plane and towards the galactic north pole; R_a is the apogalactic distance, R_p is the perigalactic distance, e is the eccentricity, and i is the mean inclination angle of the orbit plane.

7. Discussion

The space velocity and the orbital parameters of NGC 4147 in Table 10 are quite different from those given by Dauphole & Colin (1995), but are in good agreement with the values given by Odenkirchen et al. (1997). The major difference to the work of Dauphole & Colin (1995) lies in the velocity component Θ, where our values change the cluster's prograde rotation of Dauphole & Colin (1995) into a retrograde motion. Since the inclination angle of the cluster orbit is close to 90 degree, small changes in the proper motion may change the sign of Θ. Both of the absolute proper motion results from this paper and from Odenkirchen et al. (1997) are based on the Hipparcos reference frame and should have a better reliability. However, large proper motion errors of the single stars exist in the previous work while the proper motion reduced in the present work should be better due to deeper first epoch plates. From the relationship between apogalactic distance R_a and metallicity [Fe/H] of 26 globular clusters, Dauphole et al. (1996) proposed the existence of a metallicity gradient among the halo globular clusters and they took this as a support to the rapid collapse model of the Galaxy (ELS). It seems that such a metallicity gradient is present in their Fig. 4. NGC 4147 is one of the two clusters, which do not fit very well to the proposed relation. As for NGC 4147, according to Dauphole & Colin (1995), its apogalactic distance is 52 kpc, while its metallicity [Fe/H] = −1.80. If the metallicity gradient is true for the halo clusters, NGC 4147 should have an apogalactic distance smaller than 40 kpc. Using R_a calculated here or from Odenkirchen et al. (1997), the apogalactic distance of NGC 4147 will fit better to the apogalactic relation of distance and metallicity and NGC 4147 will be then a "normal" cluster. Among the smaller sample of 15 clusters with proper motions based on Hipparcos reference stars in Odenkirchen et al. (1997) the relation between R_a and [Fe/H] is hardly seen. What can be inferred from their work is that the more metal-rich clusters are concentrated towards the galactic center and that the group of clusters with retrograde orbits (including NGC 4147) is in general chemically quite homogeneous, with [Fe/H] between −1.5 to −2.0. This conclusion is to a certain extent in favor of Searle & Zinn's (1978) accretion model, but it not necessarily excludes the ELS model. Our results support the conclusion of Odenkirchen et al. (1997). Obviously more accurate absolute proper motion data of globular clusters should be obtained before we can make definite conclusion on the existence of the metallicity gradient and which of the ELS and SZ models would be the most favorable scenario for the formation of our Galaxy.

References

Allen C.W., 1973, Astrophysical Quantities, Third edition, University of London. The Athlone Press
Aurière M., Lauzeral C., 1991, A&A 244, 303
Brosche P., Geffert M., Ninkovic S., 1983, Publ. Astron. Inst., Czech. Acad. Sci. 56, 145

Brosche P., Geffert M., Klemola A.R., et al., 1985, AJ 90, 2033
Christian C.A., Adams M., Barnes J.V., et al., 1985, PASP 97, 363
Dauphole B., Geffert M., Colin J., Ducourant C., Odenkirchen M., Tucholke H.-J., 1995, A&A 313, 119
Eggen O., Lynden-Bell D., Sandage A., 1962, ApJ 136, 762 (ELS)
Friel E.D., Heasly J.N., Christian C.A., 1987, PASP 99, 1248
Geffert M., Dauphole B., Colin J., et al., 1995, Stellar Populations, IAU Symp. 164. Kluwer Academic Publishers, p. 406
Geffert M., Hiesgen M., Colin J., Dauphole B., Ducourant C., 1997, in ESA SP-402. ESA Publications Division Noordwijk, p. 579
Odenkirchen M., Brosche P., Geffert M., Tucholke H.-J., 1997, New Astron. 2, 477
Russell J.L., 1976, Ph.D. Thesis, University of Pittsburgh
Sandage A.R., Walker M.F., 1955, AJ 60, 230
Searle L., Zinn R., 1978, ApJ 225, 357 (SZ)
Stetson P.B., 1987, PASP 99, 191
Stetson P.B., 1992, IAU Coll. No. 136, "On Stellar Photometry - Current Techniques and Future Developments" Butler C.J. & Elliot I. (eds.), p. 291
Wang J.J., Chen L., Zhao J.H., Jiang P.F., 1996, CA&A 20, 364
Zhao J.H., Zhao J.L., 1994, Ann. Shang. Obs. 15, 85